FINITE ELEMENT ANALYSIS OF SOME CERVICAL SPINAL CORD INJURY MODES

L E Bilston
Department of Mechanical and Mechatronic Engineering, University of Sydney

ABSTRACT

In this study, a finite element model of the human cervical spinal column was constructed in order to investigate the effects of material parameters on the deformation patterns of the cervical spinal cord during simulated hyperflexion, hyperextension, and axial compression. In the first instance, the results from a physical model study of similar injuries were simulated. This enabled validation of the spinal motions and spinal cord deformations. Subsequently, the effects of material parameters and constitutive models on the spinal cord deformations and stresses were investigated.

THIS PAPER DESCRIBES firstly, the construction and validation of a simple two dimensional finite element model of the cervical spinal cord and vertebral column, and then the use of that model to investigate the effects of variations in material properties and constitutive models on the strain fields developed in the spinal cord during hyperflexion, hyperextension and axial compression motions. Such analysis allows us to examine how simplifications made in physical and other element models affect the response of the spinal cord tissue to deformation.

Cervical spinal cord injury (SCI), although not a common occurrence, is nevertheless a serious, expensive and debilitating injury. Spinal cord injuries occur most commonly as a result of motor vehicle, recreational and sporting accidents (Pope and Tarlov 1991). There are a wide variety of mechanisms associated with cervical spinal cord injury, including axial compression, hyperflexion, hyperextension, and combinations of these.

Little is known about the biomechanical details of the mechanical insult to the spinal cord during SCI. The accepted wisdom is that the spinal cord is damaged by intrusion of the vertebrae into the spinal canal, causing a crush injury. In traumatic brain injury, it has been shown that axons can be damaged by dynamic tensile loading (Galbraith, Thibault et al. 1993) as a result of gross

shearing of the brain. It seems reasonable to assume that the axons in the spinal cord may be also adversely affected by dynamic deformations, although the patterns of deformation of the spinal cord are not yet well understood.

Finite element models are a useful tool in studying the mechanics of complex structures, such as the spinal column, whose geometry precludes analytical modelling. Previous finite element models of the head-neck structure have been developed in order to study various specific injury modes to the vertebral column. Belytschko et al (Belytschko, Schwer et al. 1978), and Privitzer and Kaleps (Privitzer and Kaleps 1990) have constructed detailed discretized representations of the head-neck structure in order to study the pilot ejection problem. A more general adaptation of this model was reported by Williams and Belytschko (Williams and Belytschko 1983). More recently, Kleinberger (Kleinberger 1994) has developed a three dimensional finite element model of the human cervical spine, with which he has simulated axial compression of the neck and a frontal crash test. Hosey and Liu (Hosey and Liu 1982) developed the only finite element model to explicitly include a spinal cord in addition to the brain, skull and vertebral column, which was used to investigate head and brain mechanics. That model, however, uses a small displacement, linear elastic formulation, which not only restricts it to small motions and deformations, but also greatly simplifies the constitutive behaviour of the CNS tissues. No previous studies have been reported which use large deformation non-linear finite element techniques to model the mechanics of the cervical spinal cord within the vertebral canal during injury.

METHODS

A two dimensional finite element model was constructed of the cervical spinal cord, brain, and vertebral column. The analysis was conducted in two parts. The first simulations were conducted for validation purposes. In these runs, loading conditions and mechanical properties from the preceding physical model study were used, and the deformation fields in the spinal cord were compared directly to those measured in the physical model. The second series of simulations investigated the effects of material and loading parameters on the deformations experienced by the spinal cord. In this second series of runs, constitutive models more representative of the human were used. A nonlinear material model which better models the character of the spinal cord was investigated, along with the effects of varying the mechanical properties within both this and the linear model.

FINITE ELEMENT SOFTWARE - The model was developed using the PATRAN finite element preprocessor (PDA Engineering, CA), on an Alpha 4/166 workstation (Digital Equipment Corp). The ABAQUS/Standard (Hibbitt Karlsson & Sorensen, RI) finite element code was used to analyse the model, and the results were visualised with the ABAQUS/Post post processor. The use of a nonlinear dynamic formulation with large strains and geometric

nonlinearities allowed the modelling of the effects of inertial loading on the spinal cord and brain tissues.

MODEL GEOMETRY - The model geometry reproduced a 2-D mid-sagittal slice through the human head and cervical spine. Specifically, the geometry was similar to that of the physical model study described in the previous paper. The vertebral geometry was constructed by digitising the coordinates of a mid-sagittal cut through a plastic skeleton used in the construction of the physical model. The accuracy of this digitising is approximately 0.5mm. The cord structure was modelled as a uniform rectangle, imitating the cross-section of the physical model spinal cord. That is, the cord is 150mm long, and a uniform 10mm in diameter. The only geometrical simplification made for the finite element model was modelling the geometry of the skull and brain to be a circular region bounded by a rigid skull, of an inner diameter of 80mm, which represents the effective average diameter of the human skull when rotated around the head centre of gravity (Margulies, Thibault et al. 1990). The physical model, on the other hand, used a reproduction human skull. This was not expected to greatly affect the cord behaviour, since very little deformation of the brain was seen in the physical model studies. The vertebrae were modelled as rigid bodies, since their deformation is likely to be much smaller than the cord deformations. The spinal cord was not initially in contact with any of the vertebrae, having a 1.5mm clearance from the anterior vertebrae surface. This clearance was estimated from photographs of hemisectioned human cadavers reported by Brieg (Brieg 1960), and was similar to the clearance in the physical model. The percentage of the spinal canal occupied by the cord in the model is consistent with the human cadaver hemisections from Brieg's work (Brieg 1960), where the thickness of the meninges is absorbed into the cord size. The effect of the cerebrospinal fluid, which is a viscous fluid with viscosity similar to water, is simulated by using a pure slip condition at the cord-vertebra interface. ie The tangential friction coefficient is zero. The fluid lubrication effects were simulated by making this contact "softened" in the radial direction, allowing a gradual application of the contact force over a short distance rather than a sudden contact. This method treats the contact as an elastic event, where the pressure applied to the deformable spinal cord surface is linearly related to the clearance, until actual contact is made. Mathematical details of this contact formulation are described in the ABAQUS manual (1993).

The spinal cord and brain were meshed with two dimensional solid four node quadrilateral elements, and a plane strain hybrid formulation was used to enable the use of incompressible material models. The vertebrae and skull were modelled as rigid surfaces, and a smoothing algorithm in the finite element code was enabled to avoid sharp points at the ends of the bar elements. Motion of these rigid vertebral and skull surfaces was prescribed in the model, by applying displacement boundary conditions to their reference nodes. The model for axial compression was slightly different, incorporating linear elastic elements between the vertebrae to simulate the effect of the intervertebral disks and ligamenta flava, as these factors played a more

important role in compression than in flexion and extension. The vertebrae were attached to the skull by means of a linear spring.

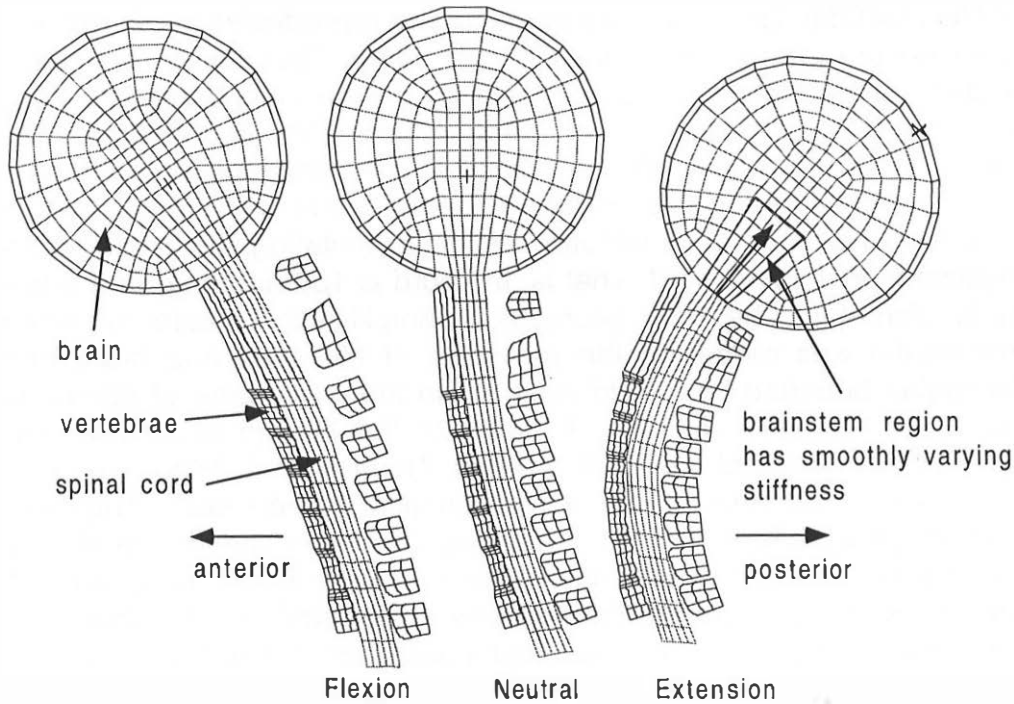

Figure 1. The mesh geometry of the two dimensional finite element model of the cervical spine and head. The model is shown in the flexed (left), normal (centre) and extended (right) positions. The spinal cord is of uniform 10mm diameter. The structure of each vertebra has been accurately reproduced on the inner canal contact surfaces. The geometry of the skull and brain has been simplified to a region bounded by a circle representing the average effective inner diameter of the human skull. Note that this schematic represents the mesh geometry, the element mesh is much finer than the grid crossings shown here. The mechanical properties of the brainstem are varied smoothly across the highlighted region as shown.

LOADING CONDITIONS - The model was loaded in such a way as to simulate the loading conditions during a hyperflexion, hyperextension, or axial compression injury, as might be expected from an automotive impact. The loading history of Ewing and Thomas (Ewing and Thomas 1972) was used to develop the head acceleration time history for the flexion and extension cases. More specifically, the exact loading history of two sets of previous physical modelling experiments (Bilston et al. 1996; Bilston and Thibault 1997) were used, so that the results of those simulations could be used to validate our finite element model. Prescribed time varying displacement boundary conditions were applied to the individual model vertebrae for flexion and extension simulations. In the case of the axial compression model, the displacement of the skull was prescribed, and the vertebral motions which occurred from the axial compression were controlled by the properties of the disk and ligamenta flava elements. The displacement loading histories for the vertebrae were

developed from a combination of the normal human vertebral kinematics, as measured by Bilston (Bilston 1994) and the measured acceleration-time history for the head from the physical model experiments in the case of the flexion and extension simulations, and from the experiments of Yoganandan et al (Yoganandan, Pintar et al. 1991), resulting in axial displacements of the head of approximately 35mm. The MRI work with volunteers showed that the rotations of each cervical vertebra is approximately linearly related to the head rotation throughout the motion. We therefore chose to apply the same *shape* vertebral rotation-time history as for the skull, but scaled the magnitude of the angular motion for each vertebra to the proportion of the head rotation measured in the abovementioned MRI study. This method was used because there is no available data in the literature which gives detailed motions of the cervical vertebrae during dynamic hyperflexion and hyperextension.

Displacement - time boundary conditions were applied to each rigid surface by means of a rigid body node, which acts as a master node for the surface. All displacement boundary conditions were applied to this node, and included displacements in the r and θ directions (relative to a coordinate system based at T1), and also rotation about the z-axis, for our two dimensional model. Rotations about the z-axis are pure rotations of the rigid surface around its own rigid body node. For the axial compression models, the skull was moved through 35mm axial displacement, over 100ms, by applying this boundary condition to the skull rigid body.

MATERIAL PROPERTIES - Two sets of simulations carried out with the finite element model used different mechanical property data. The first series of simulations was aimed at accurately reproducing the conditions of the physical model study in order to validate the finite element model. The spinal cord in the physical model is constructed of axially running Dacron fibres embedded in a linear-elastic silicone gel matrix, and so a linear elastic orthotropic material model was used for the validation simulations. The second set of simulations use both hyperelastic and isotropic linear elastic models to simulate the behaviour of a human spinal cord. The human spinal cord is nonlinear, time dependent, and anisotropic (Bilston and Thibault 1996). It exhibits the characteristic "j-shaped" stress-strain behaviour of many soft biological tissues. This type of behaviour may be modelled by the use of a hyperelastic model. The model used here is based on the large deformation hyperelastic theory of Ogden. A first order strain energy density potential function was used to define the material behaviour. The form of this potential function is:

$$U = \frac{2\mu}{\alpha^2}\left(\lambda_1^{\alpha} + \lambda_2^{\alpha} + \lambda_3^{\alpha} - 3\right) + \frac{1}{D}\left(J_{elastic} - 1\right)^2 \qquad [1]$$

where:

U = strain energy density
α, μ, D = material parameters
λ_i = principal stretch ratios
$J_{elastic}$ = elastic volume ratio.

The cord is also softer in the radial direction than in the axial direction (Bilston and Thibault 1996). This was modelled in the physical model with the use of the Dacron fibres. Unfortunately, ABAQUS does not allow the combination of both orthotropic and hyperelastic behaviour in the material model, and it was necessary to isolate the effects of the nonlinear material model from the effects of the anisotropy. Thus, in order to compare the data from the isotropic hyperelastic case to the results from the linear orthotropic case, an additional set of simulations were run with a linear elastic cord model. In all cases, the mechanical properties of the brain and spinal cord were different, and the brainstem region was modelled as a smooth transition between the two. The brainstem was modelled as a linearly flaring region, whose mechanical properties change linearly from the spinal cord stiffness to the brain stiffness from the caudal to cephalad direction. There remains, however, a sudden change in mechanical properties in the anterior-posterior directions where the brainstem meets the brain in the model. Figure 1 shows the brainstem region and the direction of changing mechanical properties.

MODEL VALIDATION - In order to arrive at an appropriate level of mesh refinement, the model was loaded repeatedly in a flexion simulation, and the mesh refined between simulations. When the peak strain in the spinal cord converged to a repeatable location and value, the mess refinement was halted, and that mesh used for further simulations. This resulted in a model with a total of 1228 quadrilateral elements and 1734 contact elements.

The model was then validated by comparing the pattern of axial strains developed in the model spinal cord with those measured in the physical model experiments, for both flexion and extension simulations. In the case of the axial compression simulations, the model was validated by comparing the vertebral displacements with those seen in the axial compression experiments.

PARAMETRIC ANALYSIS

CONSTITUTIVE EQUATIONS AND MECHANICAL PROPERTIES - The effect of using a number of different constitutive material models for the spinal cord on the spatial and temporal patterns of strain measured in the tissue was investigated, including linear-elastic, orthotropic, and hyperelastic (using an Ogden strain energy potential function for improved material model stability). The detailed definitions and derivations of these material constitutive equations may be found in the ABAQUS manual (1993). The mechanical properties (stiffness parameters) of the spinal cord were varied over a range of ±80% from the average values reported for those tissues. Data for the brain tissue was estimated as the average stiffness of brain tissue at high strain rates, from Galford and McElhaney (Galford and McElhaney 1970), and data for the spinal cord tissue was obtained from the results of the mechanical testing study of

Bilston and Thibault (Bilston and Thibault 1996). The properties for each tissue in each constitutive model are shown in Table 1.

Table 1. Mechanical properties of the brain and spinal cord.

	Spinal Cord Properties	Brain Properties
Orthotropic Cord	E11=1.2 MPa E22=0.3 MPa G12=0.23 MPa G13=0.23 MPa G23=0.18 MPa ν=0.49 ρ=1.0g/cm^3	E=0.3 MPa
Elastic Cord	E=1.2 MPa ρ=1.0g/cm^3 ν=0.49	E=0.3 MPa
Hyperelastic cord	Order (N) = 1 α=25.0 μ=0.10 ρ=1.0g/cm^3 ν=0.49	E=0.3 MPa
Viscoelastic cord	α=25.0, μ=0.10 G1,t1= 0.154,4.38 G2,t2=0.179,0.554 G3,t3=0.559,234.4	E=0.3 MPa

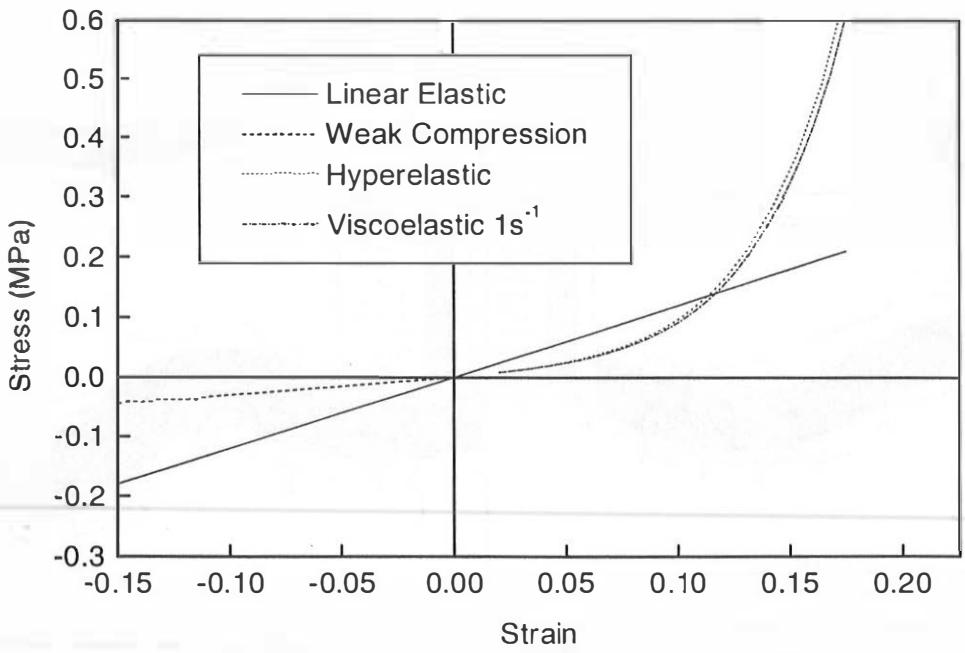

Figure 2. Comparison of stress-strain response of material models

RESULTS

VALIDATION - Flexion, extension and axial compression models were validated by direct comparison with the strain fields from the physical model study. In the physical model study, the peak strains in the spinal cord were in the range 0.2 to 0.35 in flexion, and -0.15 to 0.12 in extension. For the axial compression the flexion-compression model showed the largest strains at C2 of 0.2-0.35, and in extension-compression, the largest strains were at C5, of approximately 0.35, adjacent to the subluxing vertebra. The strains in our finite element model in flexion peaked at 0.23, which is at the lower end of the range in the physical model. There were, however, large experimental error bars in the physical model experiments, so the values measured by our simulation are consistent with that data. Moreover, the pattern of axial strains seen in our model agrees very well qualitatively with those experiments, with the largest strains in flexion being seen in the middle and upper cervical regions, while in extension, the middle cervical region shortening slightly while the upper part of the cervical cord experienced tensile strains of about 12 percent. In extension, the finite element model found a maximum strain of approximately 0.1, while some regions experienced compressive strains, similar to the physical model results. For the axial compression simulations, again good agreement between the peak strains and locations was seen. Typical patterns of strain for each type of simulation are shown in Figure 3.

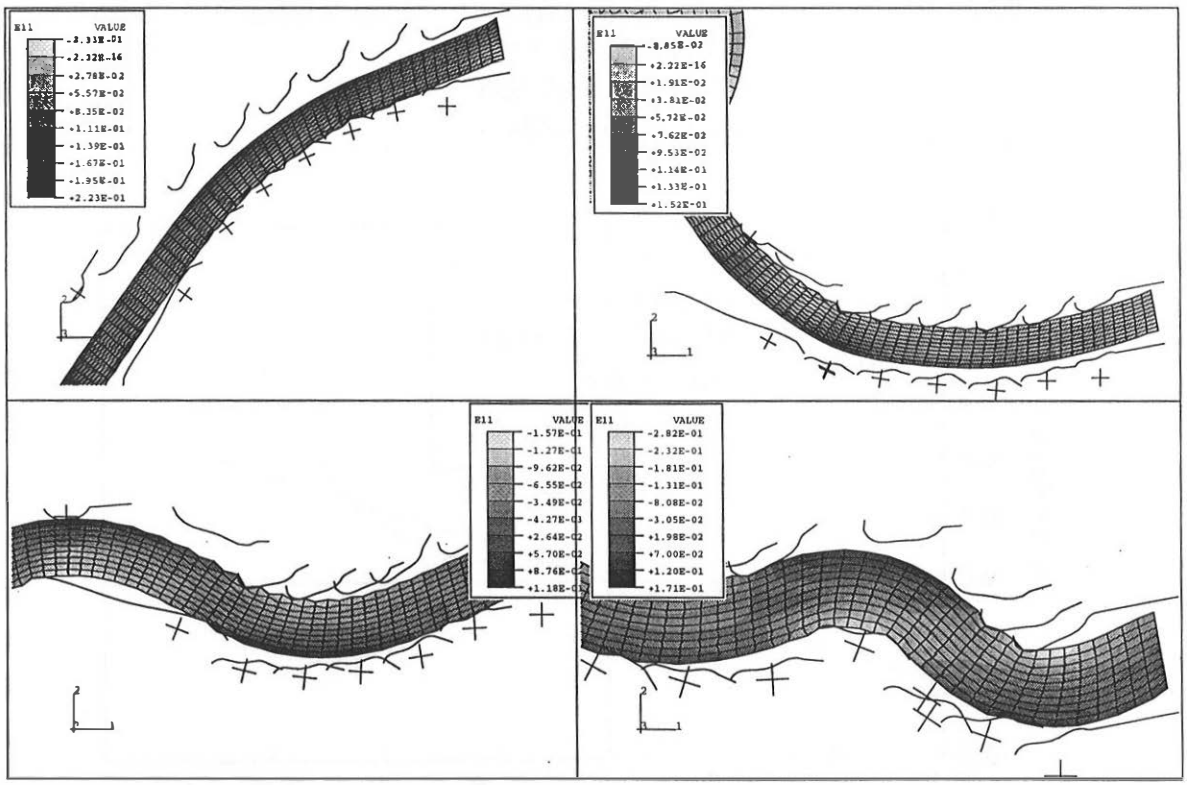

Figure 3. Spatial variation of strains and stresses in the cord during an injury simulation. (a) flexion simulation. (b) extension simulation. (c) flexion-compression (d) extension compression.

PARAMETRIC ANALYSIS - The effects of material parameters and constitutive model were investigated by parametric analysis. The effects of altering the average modulus of the spinal cord and brain in the finite element model were the first to be investigated. Large changes in the spinal cord modulus had only a slight effect on the cord strains. Corresponding changes in the cord stresses did, however, occur, with increases in cord stiffness resulting in higher stresses in the model cord. The pattern of stresses also changed somewhat, as a result of the relative softness of the brain. When the modulus was increased, the brain tended to deform more, resulting in a slight movement of the brainstem through the foramen magnum. This is probably also responsible for the slight decrease in overall cord strain with increased cord stiffness.

The effect of the constitutive model used had a more noticeable effect on the cord deformation and particularly the cord stresses. A hyperelastic model resulted in slightly increased peak strains (by approximately 3-6%) in the axial compression models, but lower strains (9-11%) in the flexion and extension simulations. The use of an isotropic linear elastic cord model had a more marked effect on the cord strains. An increase in peak cord strains of up to 19% was seen for the extension-compression simulations. The values for peak strain, strain rate and stress are given in Table 2. The associated stresses were more sensitive to the constitutive model, due to variations in strain between cord regions. That is, regions of low strain had lower stresses, and regions of high strain had higher stresses in the hyperelastic and viscoelastic models. This is expected due to the "j-shaped" stress-strain curve of these materials, where above strains of about 15%, stresses increase sharply. It is also interesting to note that the viscoelastic time-dependence did not significantly change the cord stresses and strains. This can be seen by comparing the hyperelastic and hyperelastic/viscoelastic simulation results. This suggests that the cord is behaving largely elastically during these impact loadings, and that there is little time for relaxation to occur.

DISCUSSION

The finite element model used for these simulations is a very simple one. It has been used for parametric analysis of a previous series of tests with a physical model of the human head and spinal column. As such, the finite element model includes only structures which were present in the physical model. The effects of nerve roots, dentate ligaments, the ligamenta flava etc, on the spinal cord deformations have not been investigated here. This model represents a *first order approximation* of the biomechanics of the spinal cord during injury, and further refinements will be made in future to improve the model, and to include the biomechanics of the vertebrae explicitly. This will allow simulation of a much wider range of spinal cord injury modes, particularly those for which we do not know, a priori, the vertebral displacement histories.

Table 2 Summary of results for all runs, showing changes in parameter values relative to the reference run, with the orthotropic cord model.

Run Type[1]	Constit-utive model [2]	Cord modulus (MPa)	Brain modulus (MPa)	Change in Peak Strain (%)	Change in Peak Strain Rate (%)	Change in Peak Stress (MPa)
F	OR	1.2/0.3 [3]	0.3	-	-	-
F	LE	1.2	0.3	+3	+20	+28
F	HE	- [4]	0.3	-11	-10	+330
F	HE	1.2T/0.3C[5]	0.3	-8	-10	+210
F	HE/V		0.3	-6	+9	+340
E	OR	1.2/0.3	0.3	-	-	-
E	LE	1.2	0.3	+5	+14	+20
E	HE	-	0.3	-9.5	-1.5	+37
E	HE	1.2T/0.3C	0.3	0	+7.5	+115
E	HE/V		0.3	-9.5	-1.5	+37
FC	OR	1.2/0.3	0.3	-	-	-
FC	LE	1.2	0.3	+7	-9	+23
FC	HE	-	0.3	+4	-22	+12
FC	HE	1.2T/0.3C	0.3	+12	-18	+110
FC	HE/V		0.3	+4	-22	+12
EC	OR	1.2/0.3	0.3	-	-	-
EC	LE	1.2	0.3	+19	+20	+40
EC	HE	-	0.3	+6	0	+200
EC	HE	1.2T/0.3C	0.3	+18	+50	+247
EC	HE/V		0.3	+6	0	+202

The model geometry approximates the human spine geometry, with similar clearance between the vertebrae and cord to that seen in cadaver studies (Brieg, 1960), and a cylindrical brain, with diameter equivalent to the human head in the saggital plane (see Margulies et al, 1990). The cerebrospinal fluid is not modelled explicitly, but its effects are accounted for by the use of a pure-slip condition at the cord-vertebra interface, and a softened radial contact model.

Five different material constitutive models (an orthotropic model with softer radial stiffness, an isotropic linear elastic, a model with decreased compressive stiffness, a hyperelastic model, and a hyperelastic/viscoelastic model) were examined. The human spinal cord is probably a combination of the first and last of these models, with the viscoelastic behaviour being more important at lower loading rates than those simulated here. It seems that the nonlinear orthotropic mechanical structure of the spinal cord may contribute to its protection from

[1] F=flexion, E=extension, FC=flexion-compression, EC=extension-compression

[2] LE = linear elastic, OR = orthotropic, HE = hyperelastic.

[3] Values shown for the orthotropic model are the axial and radial moduli respectively.

[4] For the hyperelastic case, the model was fitted to test data from Bilston et al (1996).

[5] In this case, a hyperelastic model was use to approximate linear elastic behaviour with different compression and tension moduli, to represent the true behaviour of the spinal cord.

mechanical injury by allowing it to absorb radial strains more easily, as evidenced by the lower strains and stresses in the orthotropic model results. The "wavy" nature of the fibre tracts gives rise to a hyperelastic behaviour, and perhaps this may protect the neural fibres from injury at lower strains.

The results from this parametric analysis also suggest that previous physical modelling work may have slightly overestimated the strains (and thus the injury risk) in the spinal cord during hyperflexion, hyperextension and axial compression.

CONCLUSIONS

In this study, we have constructed and validated a two dimensional finite element model of the mid-sagittal plane of the head and neck during hyperflexion and hyperextension. The model geometry and loading conditions reproduce those of a previous physical model of these types of injuries. The results from that physical model study were used to validate the strain patterns in the finite element model. The model was then used to investigate the effects of loading parameters and material parameters on the spinal cord deformation. The key findings were that the use of a linear orthotropic spinal cord surrogate in the previous physical model study, rather than a hyperelastic orthotropic one similar to the human spinal cord may have resulted in a small overestimation of the strains experienced by the spinal cord during hyperflexion and hyperextension.

REFERENCES

(1993). ABAQUS Theory Manual, v5.3. Pawtucket, RI, Hibbett, Karlsson, and Sorensen, Inc.

Belytschko, T., L. Schwer, et al. (1978). "Theory and application of a three-dimensional model of the human spine." Aviat Space Environ Med **49**(1 Pt. 2): 158-65.

Bilston, L. E. (1994). The biomechanics of the spinal cord during traumatic spinal cord injury. Bioengineering. Philadelphia, University of Pennsylvania.

Bilston, L. E., M. Griffiths, J. Brown (1996). Biomechanics of the cervical spinal cord in rollover crashes. 15th International Technical Conference on Enhanced Safety of Vehicles, Melbourne, Australia, US D.O.T.

Bilston, L. E. and L. E. Thibault (1996). "The mechanical properties of the human cervical spinal cord in vitro." Annals of Biomedical Engineering **24**(1): 67-74.

Bilston, L. E. and L. E. Thibault (1997). "Biomechanics of cervical spinal cord injury in flexion and extension: A physical model to estimate spinal cord deformations." International Journal of Crashworthiness **2**(2): 207-218.

Brieg, A. (1960). Biomechanics of the central nervous system. Stockholm, Almqvist and Wiksells.

de Jager, M., A. Sauren, et al. (1994). Three-dimensional head-neck model: validation for frontal and lateral impacts. Stapp, Sae.
Ewing, C. L. and J. T. Thomas (1972). Human head and neck response to impact acceleration. Pensacola, FL, Naval Aerospace Medical Research Laboratory.
Galbraith, J. A., L. E. Thibault, et al. (1993). "Mechanical and electrical responses of the squid giant axon to simple elongation." Journal of Biomechanical Engineering **115**: 13-22.
Galford, J. E. and J. H. McElhaney (1970). "A Viscoelastic Study of Scalp, Brain, and Dura." J. Biomechanics **3**: 211-221.
Hosey, R. R. and Y.-K. Liu (1982). A homeomorphic finite element model of impact head and
neck injury. Finite Elements in Biomechanics. R. H. C. e. al, John Wiley and Sons, Ltd: 379-401.
Huelke, D. F., G. M. Mackay, et al. (1992). "Car crashes and non-head impact cervical spine injuries in infants and children." SAE Technical Paper Series: 1-6, paper 920652.
Huelke, D. F., G. M. Mackay, et al. (1992). "Non-head impact cervical spine injuries in frontal car crashes to lap-shoulder belted occupants." SAE Transactions: paper 920560.
Kleinberger, M. (1994). Application of finite element techniques to the study of cervical spine mechanics. Stapp, Sae.
Margulies, S. S., L. E. Thibault, et al. (1990). "Physical Model Simulations of Brain Injury in the Primate." J Biomechanics **23**(8): 823-836.
Pope, A. M. and A. R. Tarlov (1991). Prevention of Injury-Related Disability. Disability in America: Toward an National Agenda for Prevention. Washington, D.C., National Academic Press: 147-183.
Privitzer, E. and I. Kaleps (1990). Effects of head-mounted devices on head-neck dynamic
response to +Gz accelerations. *Neck Injury in Advanced Military Aircraft Environment,* AGARD Conference Proceedings.
Williams, J. L. and T. B. Belytschko (1983). "A Three-Dimensional Model of the Human Cervical Spine for Impact Simulation." J Biomech Eng **105**: 321-331.
Yoganandan, N., F. A. Pintar, et al. (1991). "Strength and Kinematics Response of Dynamic Cervical Spine Injuries." Spine **16**(10 Suppl): S511-517.

ACKNOWLEDGEMENTS

This work has been supported in part by University of Sydney Research Grant U0836.